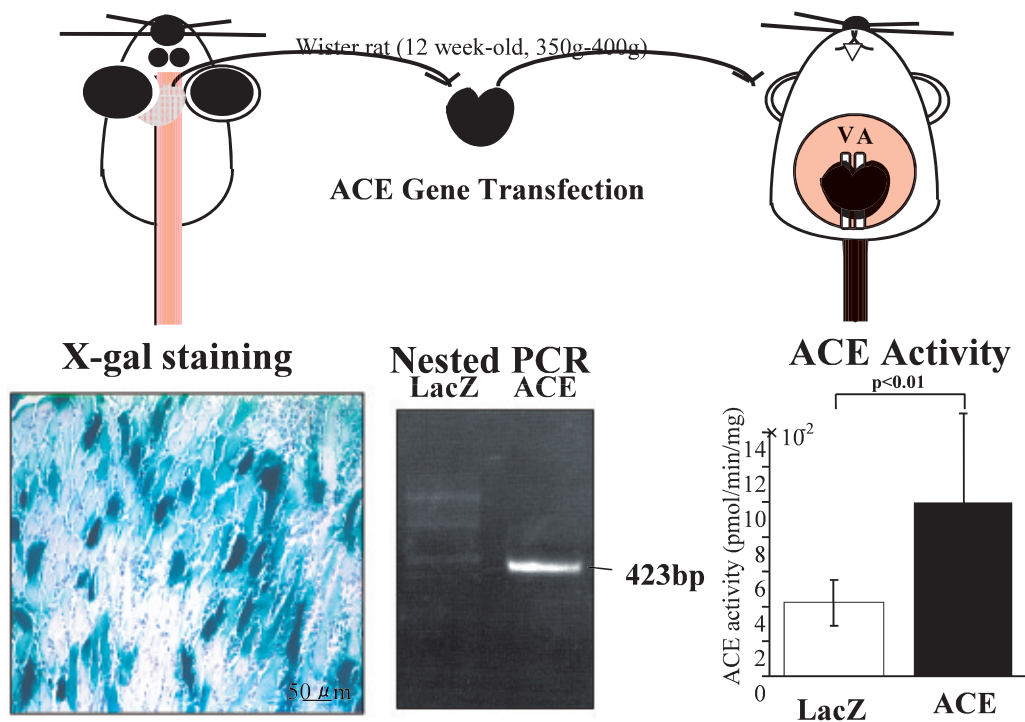


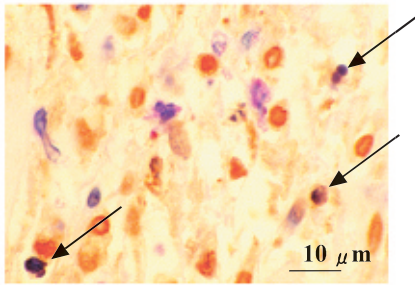
Color Fig. 1 Upper two panels: Representative cross sectional views obtained from control F1b and BIO hamsters at the age of 26 weeks. Lower two panels: Photomicroscopic findings ($\times 300$) of left ventricles of BIO (right panel) and F1b (left panel). Sections are stained by PAS-hematoxylin. Bar denotes a length of $20\mu\text{m}$. Chapter 1, p.6



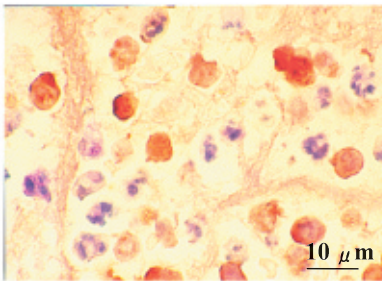
Color Fig. 2 Upper Panel: Schematic view of an in-vivo system for the human ACE gene transfection using an adenovirus vector. The heart was removed from the donor 12 week of age Wistar rat and the human ACE or LacZ gene was transfected, then the heart was transplanted into the abdominal aorta and inferior vena cava of another rat. Lower Panel from left to right: X-gal staining, nested PCR and ACE activity. X-gal staining was performed 3 weeks after heart transplantation. Probe for nested PCR is used a human ACE gene fragment. Left ventricular ACE activity in LV expressed by nmol/mg protein. Chapter 1, p.8

TUNEL Staining

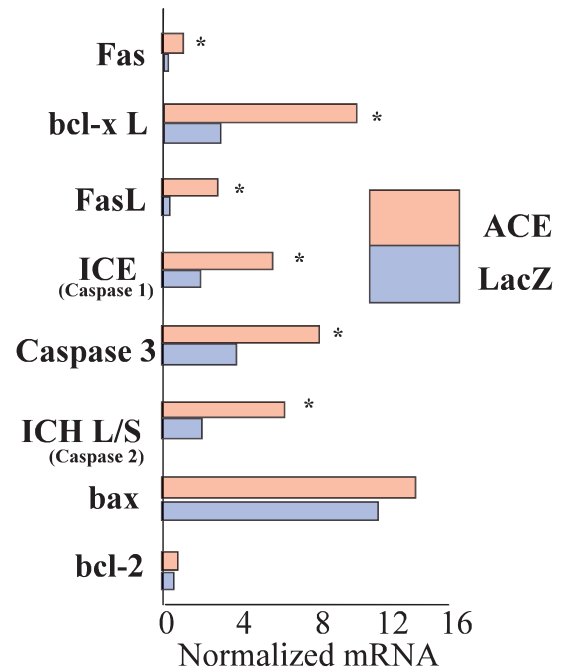
AdxACE



AdxLacZ



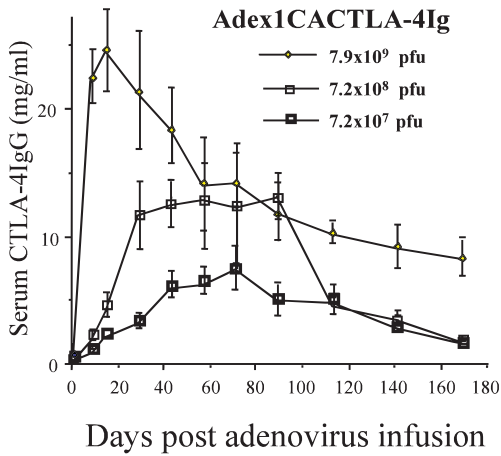
Apoptosis Related Gene Expressions (Multi-Probe RPA)



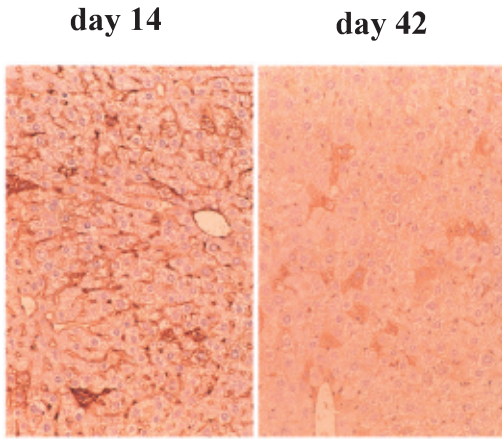
Color Fig. 3 Left Panel: Photomicrographs of in situ TUNEL staining 3 weeks after ACE (upper) or LacZ (lower) transfection. TUNEL positive myocytes can be seen 2-3 in the field ($\times 300$) as indicated by arrows in the ACE transfected heart.

Right Panel: Apoptosis related gene expression for Fas, bclxL, FasL, ICE, Caspase 3, Caspase 2, bax and bcl-2 detected by multi-probes nuclease protection assay. Chapter 1, p.9

**Serum Concentrations
of CTLA-4Ig**
(After IV Injection of AdexCTLA-4Ig)



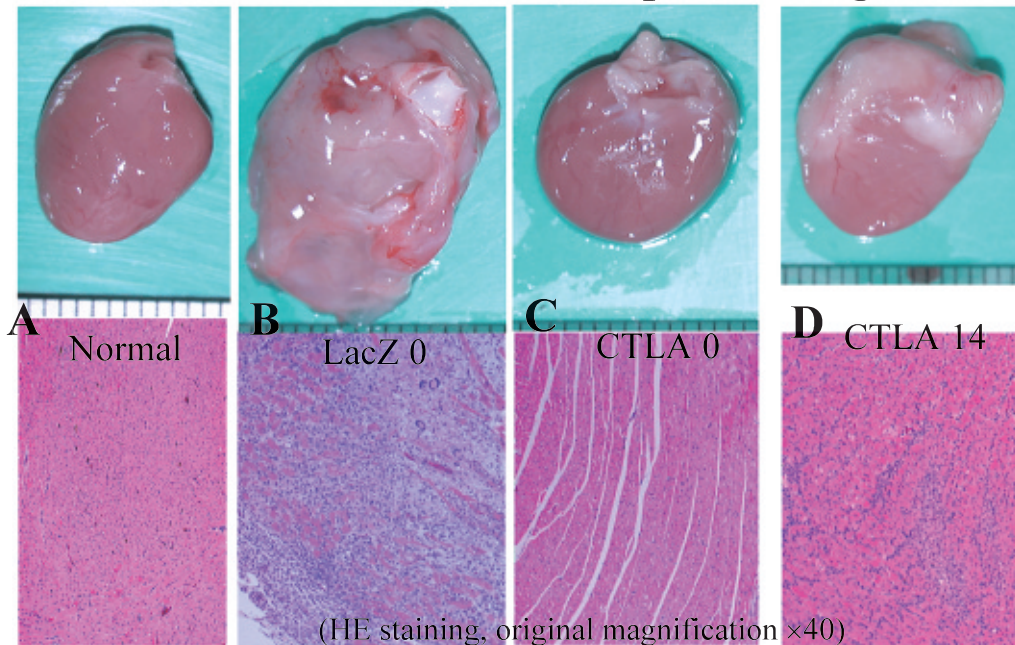
**In Situ Production
of CTLA4-Ig in Liver**



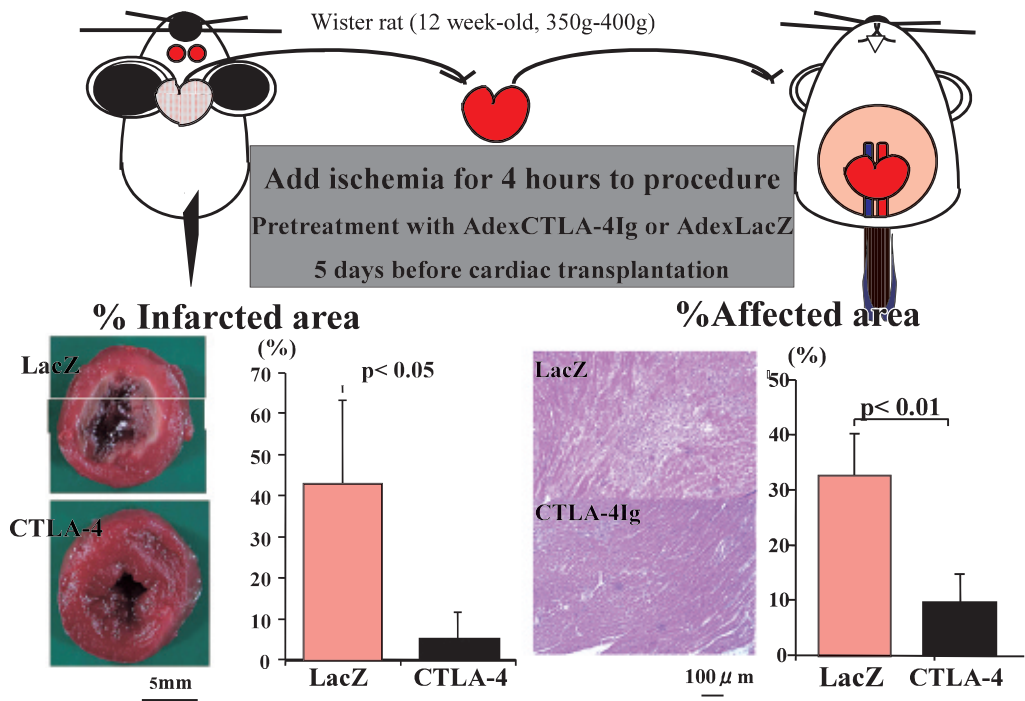
Color Fig. 4 Left Panel: Serum concentrations of CTLA4Ig after gene transfer. Sera from animals treated with AdexCTLA4Ig on day 0 (n=8) was harvested at the indicated time points and analyzed by ELISA. Values represent means \pm SE.

Right Panel: Photomicrographs of In Situ production of CTLA4-Ig in Liver. Immunostaining by a murine anti-rat CTLA4 monoclonal antibody (MAb) was performed. A goat anti-rat GL50 polyclonal antibody (PAb) specifically recognizing rat was purchased from Santa Cruz Biotechnology (Santa Cruz, CA, U. S. A). Chapter 1, p.19

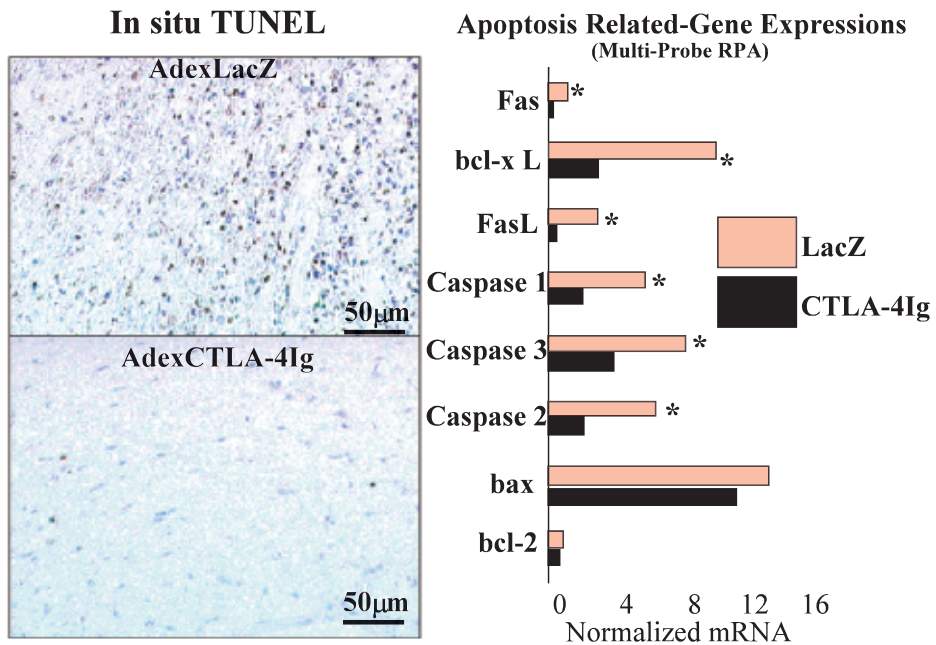
Macro- and Micro-scopic Findings



Color Fig. 5 Representative histology of cardiac tissues from rats treated with Adex-LacZ on day 0 (A), AdexCTLA4Ig on day 0 (B), AdexCD40Ig on day 0 (C), both AdexCTLA4Ig and AdexCD40Ig on day 14 (D), AdexCTLA4Ig on day 14 (E), and AdexCD40Ig on day 14 (F). All control rats treated with AdexLacZ developed typical severe autoimmune lesions in their hearts. The lesions were composed of various inflammatory cells, including multinucleated giant cells, macrophages, lymphocytes, and degenerated myocardial tissue (Fig. 15A). There was very little infiltration of inflammatory cells if any in the myocardium in the AdexCTLA4Ig- and AdexCD40Ig-treated groups on day 0 (Fig. 15B and 15C). Minimal myocarditis was observed in the group treated with a combination of AdexCTLA4Ig and AdexCD40Ig-treated group on day 14 (Fig. 15D) or AdexCTLA4Ig-treated group on day 14 (Fig. 15E) and moderate myocarditis was observed in the AdexCD40Ig-treated group on day 14 (Fig. 15F). (hematoxylin-eosin staining, original magnification $\times 40$) Chapter 1, p.20

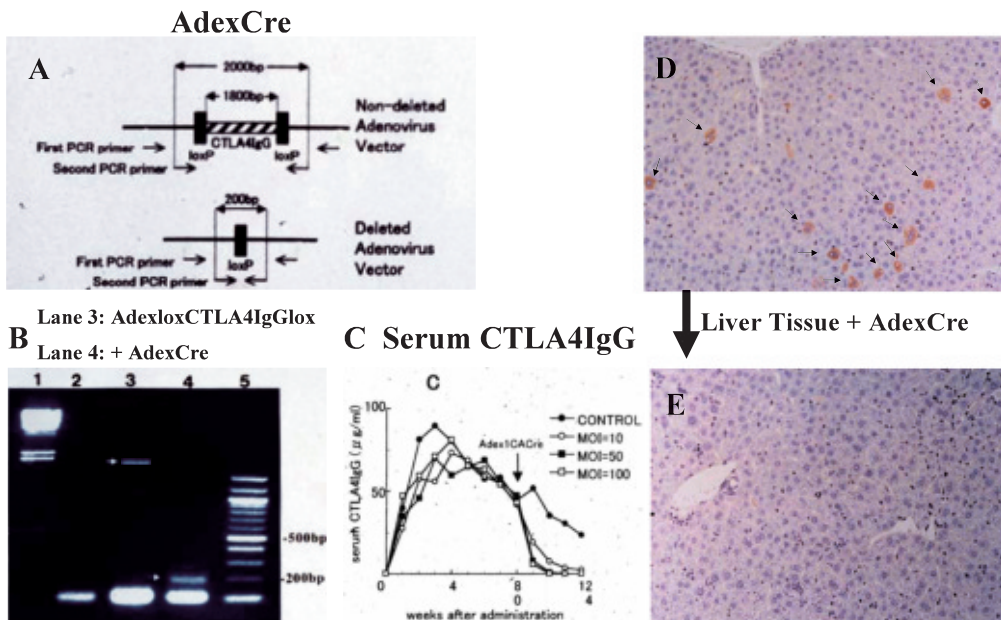


Color Fig. 6 Upper Panel: Schematic view of an in-vivo system. Ischemic time at 4 hours adding to the procedure and investigated the protective effect of CTLA4Ig against the immune response caused by reperfusion after transplantation. Hearts were transplanted into a heteropoietic location in recipients after ischemia in St. Thomas solution for 4 hours. Lower Panel from left to right: infarcted area as determined by triphenyl tetrazolium chloride (TTC) staining and affected area, evaluated on the basis of the extent of inflammatory cell infiltration. Chapter 1, p.23

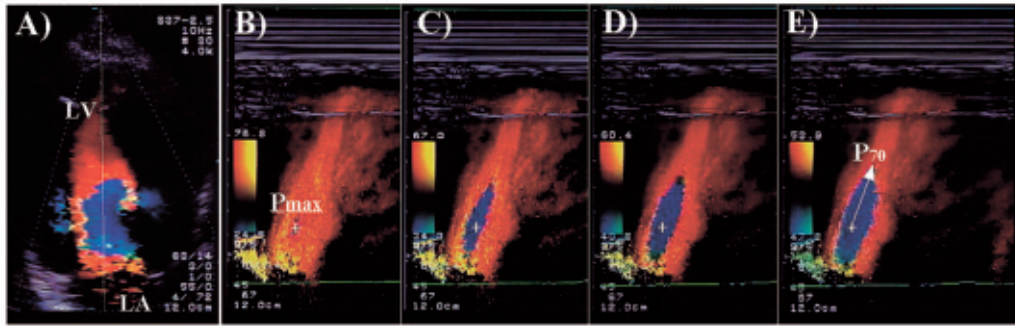


Color Fig. 7 Left Panel: Photomicrographs of in situ TUNEL staining 3 weeks after LacZ (upper) or CTLA4Ig (lower) transfection. Right Panel: Apoptosis related gene expression for Fas, bclxL, FasL, ICE, Caspase 3, Caspase 2, bax and bcl-2 detected by multi-probes nuclease protection assay. Chapter 1, p.24

Termination of CTLA-4IgG Expression by Cre Recombinase

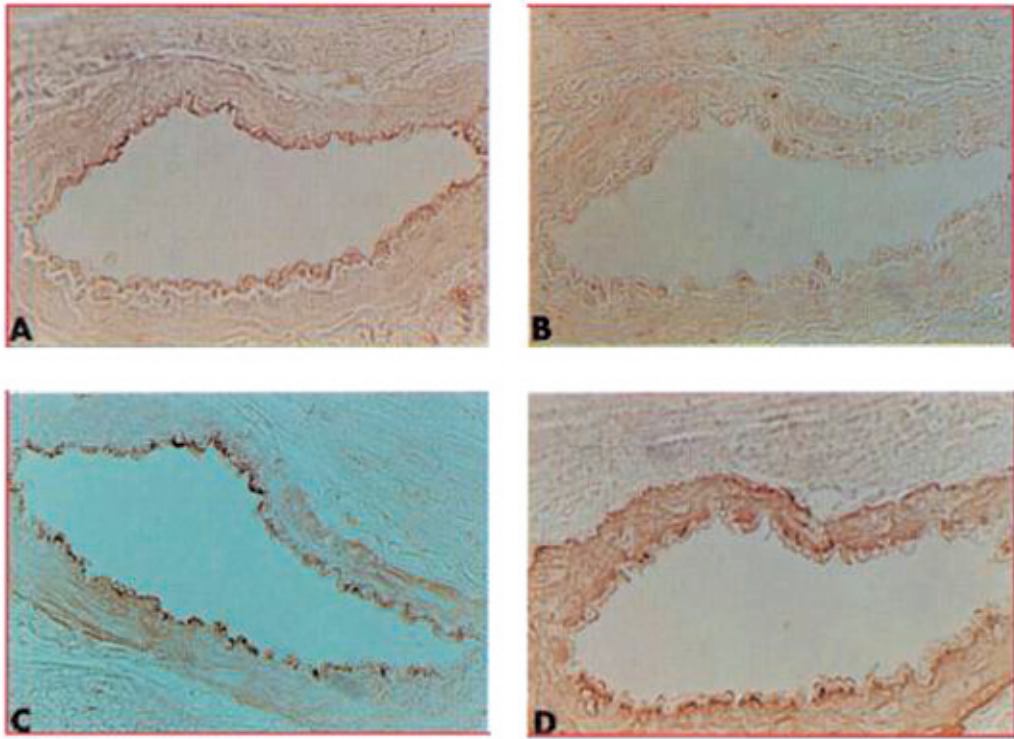


Color Fig. 8 Termination of CTLA-4IgG Expression by Cre Recombinase. Chapter 1, p. 24

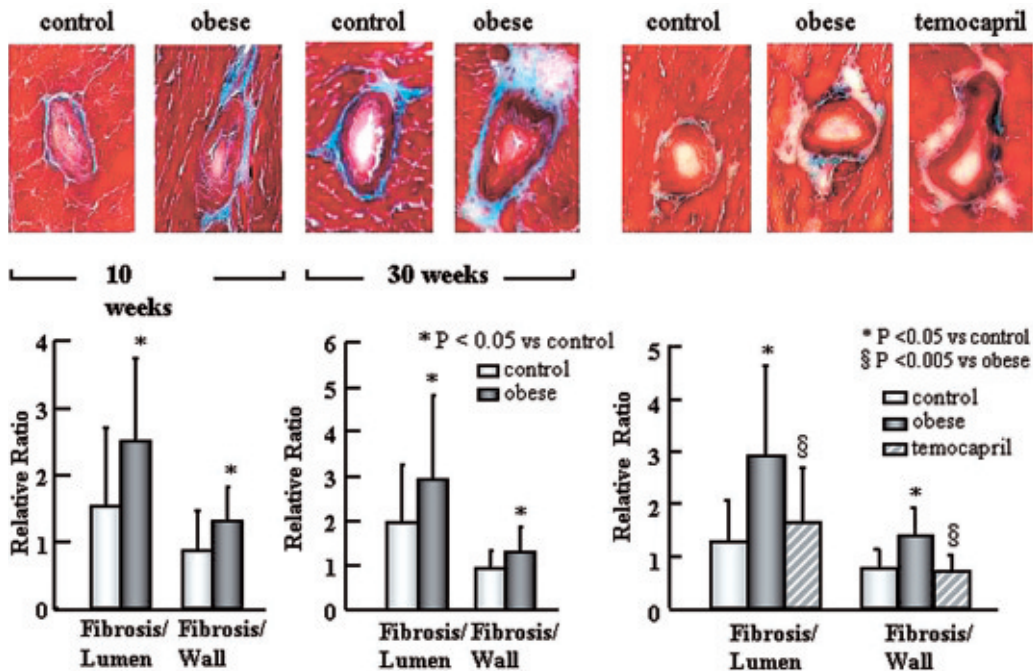


Color Fig. 9 Our method to measure flow propagation velocity using color M-mode Doppler and color baseline-shift technique.

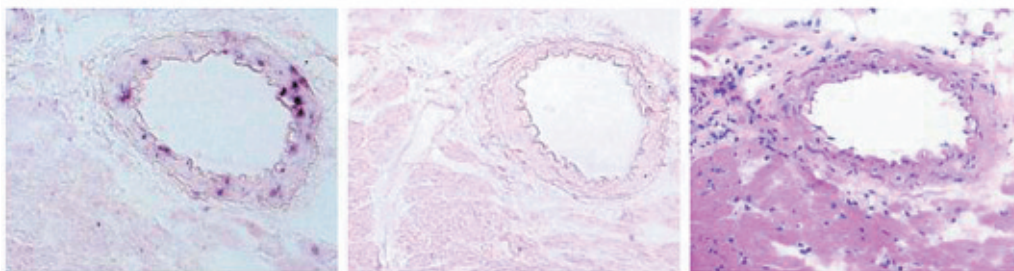
A color M-mode Doppler image of left ventricular filling flow was recorded by putting M-mode cursor along of the filling flow on the apical long-axis color Doppler image (panel A). Changing the aliasing area, we located the maximal velocity point around the mitral orifice in early diastole (Lmax, panel B). Then, the aliasing area was extended by reducing aliasing velocity (panel C and D). In the color M-mode image with the aliasing velocity decreased to 70% of the maximal velocity, the point nearest to the transducer in the aliasing area (L70, panel E) was determined. Flow propagation velocity (FPV) was measured as the upward slope of the line between these two points. LA; left atrium, LV; left ventricle. Chapter 2, p.39



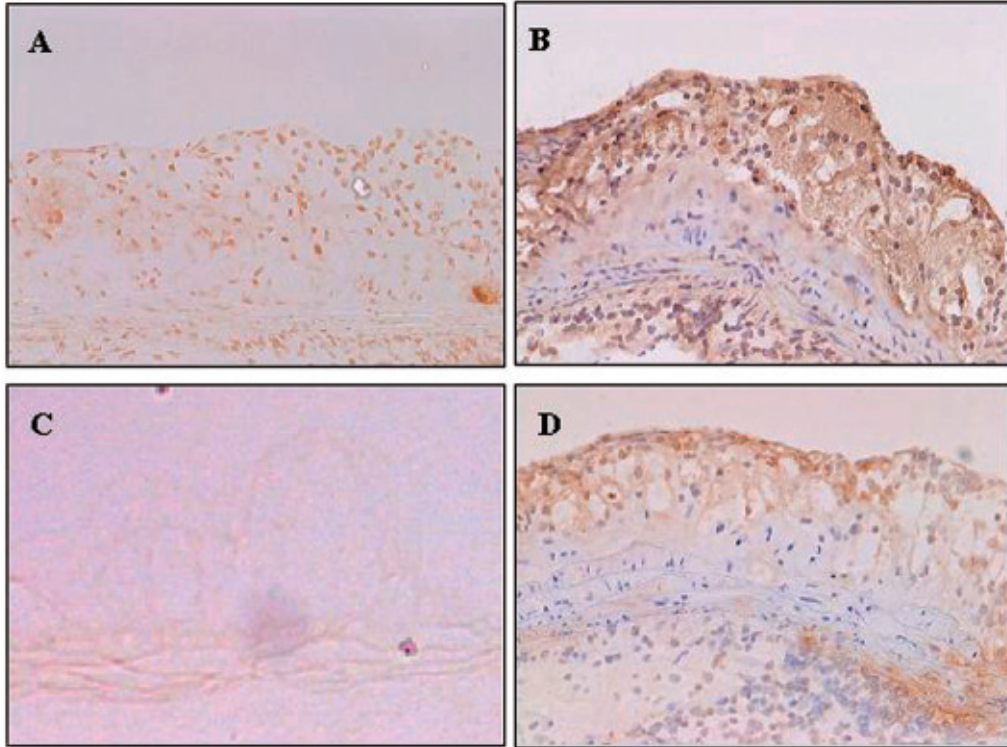
Color Fig. 10 Effects of IL-1 on PAI-1 in rat heart sections fixed in ethanol. Rats were injected with IL-1 ($1 \mu\text{g}/\text{kg}$) 24 hr before being anesthetized. The heart was perfused with phosphate buffered saline in situ and removed for analysis of PAI-1. **A:** A section of heart 24 hr after injection of IL-1 stained with rabbit antibody to PAI-1 showing specific staining in the microvascular endothelium in the myocardium. **B:** A contiguous section (control) stained with normal rabbit IgG. Microvascular endothelial cells showed no specific staining. **C:** A section contiguous with that in A stained with antibody to factor VIII related antigen indicates that cells positive for PAI-1 in A are endothelial cells positive for Factor VIII. **D:** A section contiguous to that in A stained with antibody to α -actin identifying smooth muscle cells in the tunica media. Figures quoted in part from reference 2. Chapter 3, p.56



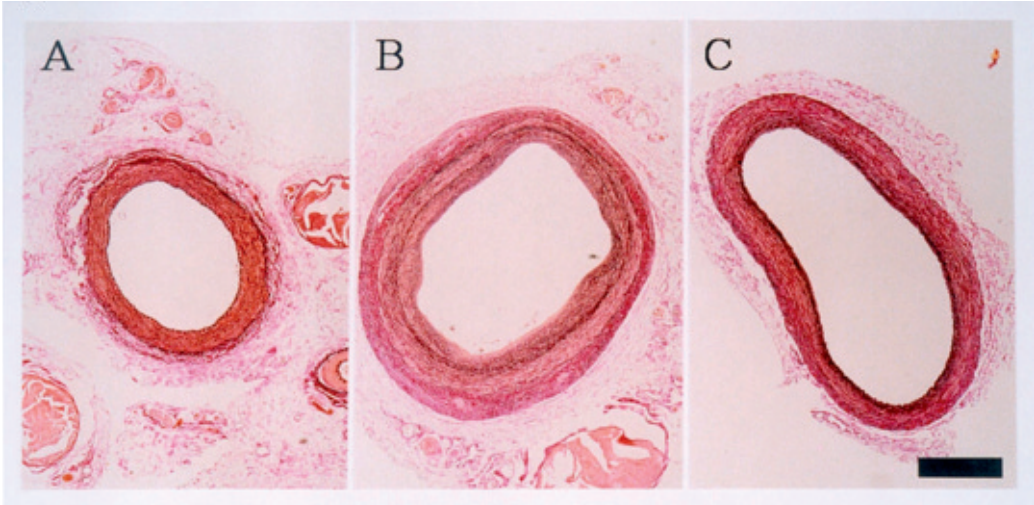
Color Fig. 11 Left: Fibrosis to lumen ratio and fibrosis to wall ratio of coronary arteries with internal diameter of less than 100 μ m in control lean and obese mice at 10 and 30 weeks. * $p < 0.05$ compared to control. (Inset) A representative photograph of coronary arteries in control and obese mice. Right: Fibrosis to lumen ratio and fibrosis to wall ratio of coronary arteries with internal diameter of less than 100 μ m in control lean, obese and obese mice treated with temocapril at 20 weeks. * $p < 0.05$ compared to control. § $p < 0.05$ compared to untreated obese mice. (Inset) A representative photograph of coronary arteries in control, obese and obese mice treated with temocapril. Figures quoted in part from reference 31. Chapter 3, p.81



Color Fig. 12 Representative photographs of in situ hybridization of the cardiac cross-sections for PAI-1 mRNA. In the left panel purple stain represents PAI-1 mRNA. The middle panel shows the negative control with sense-probe. In the right panel the section was counterstained with hematoxyline to show nuclei in dark blue. Figures quoted in part from reference 31. Chapter 3, p.81

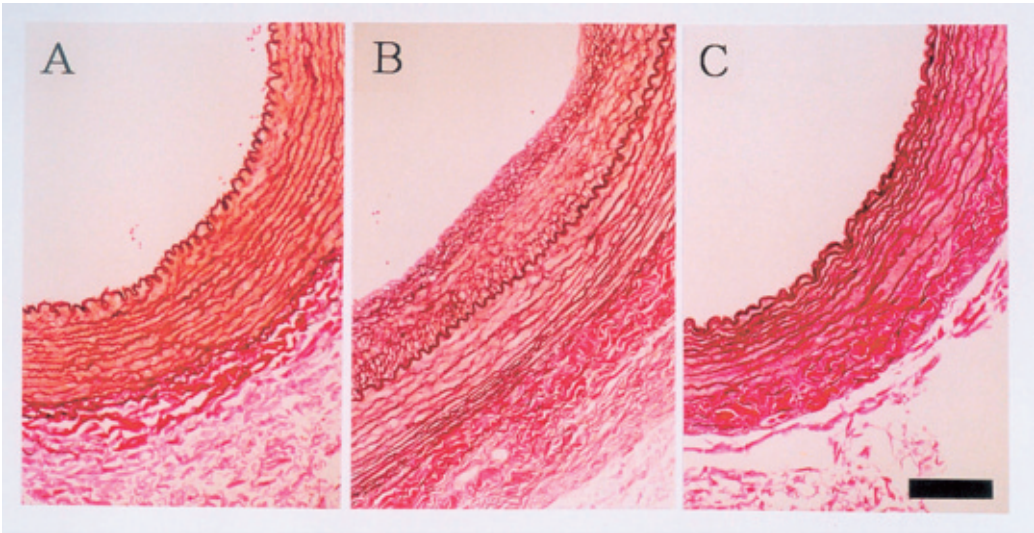


Color Fig. 13 Immunohistochemistry of the aortic atherosclerotic area from apoE^{-/-} mice for AIF-1 expression. Sections were stained for AIF-1 (A), MOMA-2 for macrophages (B) and α -actin for smooth muscle cells (D). Sections from control mouse were also stained for AIF-1 (C). Expression of AIF-1 is detected in macrophages and smooth muscle cells. Original magnifications: x100. Chapter 3, p.89



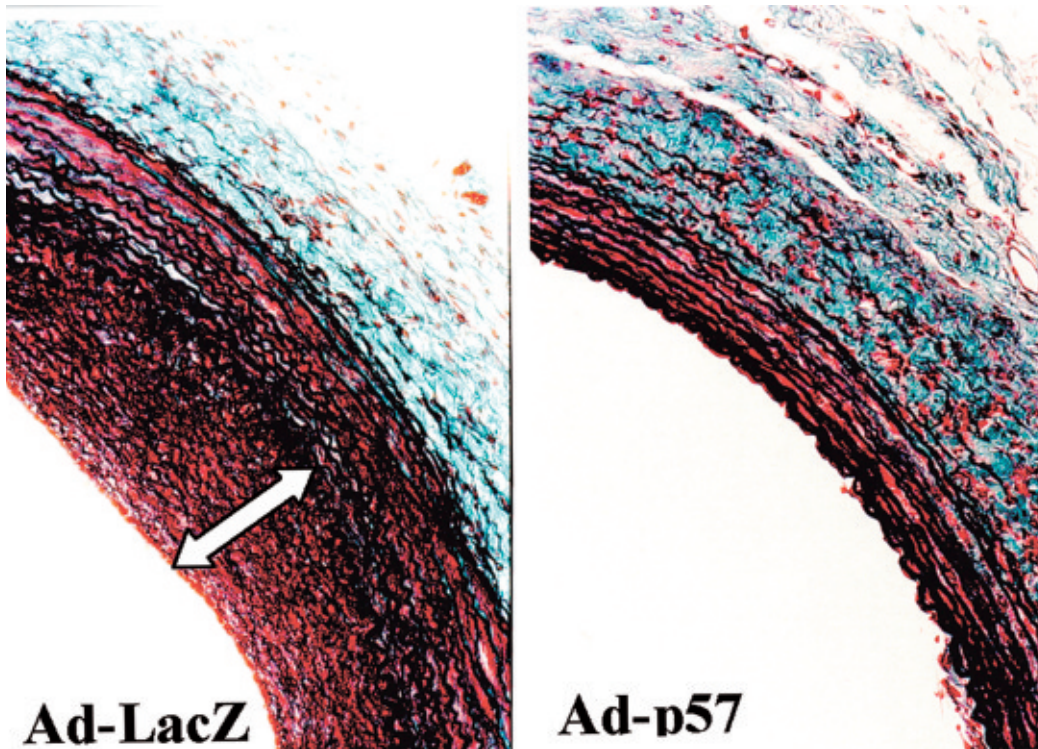
Color Fig. 14 Representative histological sections of rabbit common carotid arteries 3 weeks after balloon-mediated vascular injury (Low magnification)

Elastica Vangieson staining of representative section of rabbit carotid arteries. (A) Control carotid artery without denudation. (B) Balloon injured rabbit carotid artery treated with 5% glucose. (C) Balloon injured carotid artery treated with 1mM suramin. Black bar indicates 500mm.



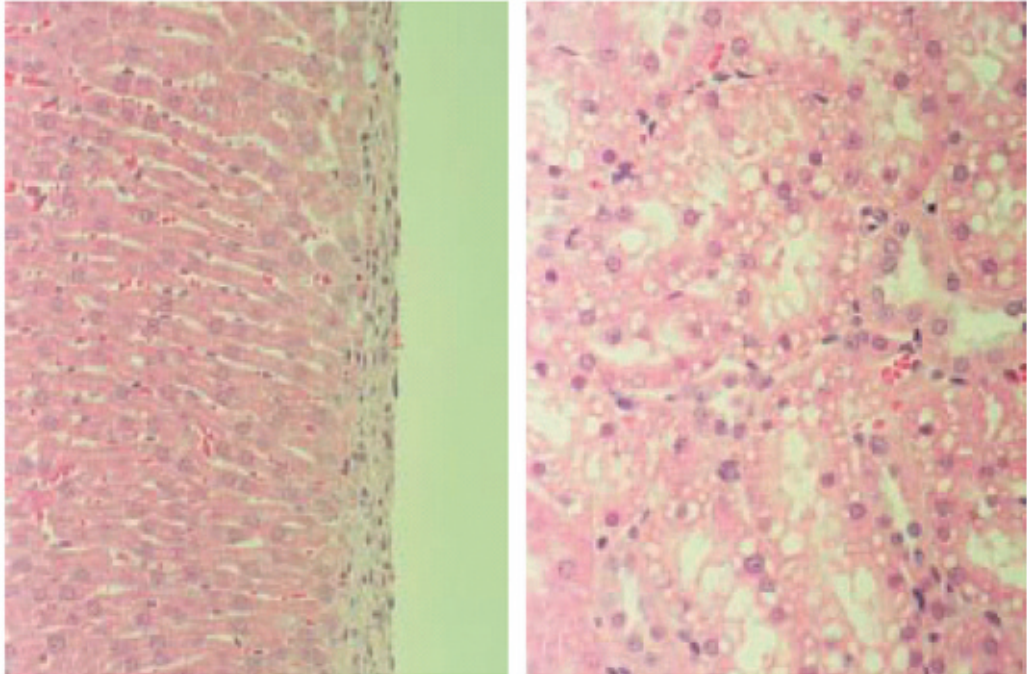
Color Fig. 15 Representative histological sections of rabbit common carotid arteries 3 weeks after balloon-mediated vascular injury (High magnification)

Representative sections of rabbit carotid arteries with higher magnification. (A) Control rabbit, (B) 5% glucose, (C) 1mM suramin injected rabbit. Black bar indicates 100mm. Chapter 4, p.110



Color Fig. 16 Effect of locally delivered Ad-p57 on neointimal formation of rabbit carotid artery

Common carotid arteries of Japanese white rabbits were injured by a inflated 3mm balloon catheter. Adenovirus constructs containing p57Kip2 gene (Ad-p57) were locally delivered and the denuded arterial segments were incubated with the adenovirus for 20min. Three weeks after the procedure, the carotid artery was excised and stained with Masson-trichrome stain. Adenovirus constructs containing bacterial LacZ gene (Ad-LacZ) were used in control rabbits. A representative section was shown in this figure. In the arterial section of control rabbit (left figure), balloon-induced neointimal formation was indicated by a white arrow. Chapter 4, p.114



Color Fig. 17 Light microscopic examination of liver (left, x 66) and kidney (right, x 100) of rats treated with SNO-PEG-Hb at 7 days postinfusion. Hematoxylin and eosin stain. Chapter 5, p.147